Sensory neuronal sensitisation occurs through HMGB-1/ RAGE and TRPV1 in high glucose conditions.

[1]Bestall S M, [3]Hulse R P, [1]Blackley Z, [1,2]Swift M, [3,4†]Ved N, [1]Paton K, [1,2]Beazley-Long N, [3]Bates D O, [1,2]Donaldson L F*.

[1]School of Life Sciences, [2]Arthritis Research UK Pain Centre, The Medical School QMC, University of Nottingham, Nottingham NG7 2UH. [3]Cancer Biology, School of Clinical Sciences, University of Nottingham, Nottingham NG7 2UH, and [4]Institute of Ophthalmology, 11-43 Bath St, London EC1V 9EL.

* Corresponding author

Email: Lucy.Donaldson@nottingham.ac.uk

Tel: (+44) 0115 8230158

[†]current address: Dept. Physiology, Anatomy and Genetics, University of Oxford, South Parks road, Oxford OX1 3PT

Author contributions

Conceptualisation: SMB, RPH, NV, NBL, ZB, MS, DOB & LFD; Methodology: SMB, ZB, RPH, NBL, DOB, LFD; Investigation: SMB, RPH, ZB, MS, NV, KP, NBL; Formal analysis: SMB, LFD. Funding acquisition: LFD, DOB, RPH; Resources: LFD, DOB, RPH; Project administration: LFD, DOB, RPH, SB; Supervision: LDF, DOB, RPH; Writing – original draft; SMB, LFD; Writing –

JCS Advance Online Article. Posted on 21 June 2018

review and editing; SMB, LFD, DOB, RPH, NBL, ZB, MS, NV. All authors have seen and approved the final version of the manuscript.

Summary statement

In high glucose conditions, nociceptive neurons are sensitised through the actions of HMGB1 acting though RAGE and PKC. This sensitisation is blocked by a vascular endothelial growth factor splice variant.

Abstract

Many potential causes for painful diabetic neuropathy have been proposed including actions of cytokines and growth factors. High mobility group protein B1 (HMGB1) is a RAGE agonist, increased in diabetes, that contributes to pain by modulating peripheral inflammatory responses. HMGB1 enhances nociceptive behaviour in naïve animals through an unknown mechanism. We tested the hypothesis that HMGB1 causes pain through direct neuronal activation of RAGE and alteration of nociceptive neuronal responsiveness. HMGB1 and RAGE expression were increased in skin and primary sensory (DRG) neurons of diabetic rats at times when pain behaviour was enhanced. Agonist-evoked TRPV1-mediated calcium responses increased in cultured DRG neurons from diabetic rats and in neurons from naïve rats exposed to high glucose concentrations. HMGB1-mediated increases in TRPV1-evoked calcium responses in DRG neurons were RAGE and PKC-dependent, and this was blocked by co-administration of the growth factor splice variant, VEGF-A_{165}b. Pain behaviour and DRG RAGE expression increases were blocked by VEGF-A_{165}b treatment of diabetic rats *in vivo*.

HMGB-1-RAGE activation sensitizes DRG neurons *in vitro*. VEGF-A_{165}b blocks HMGB-1/RAGE DRG activation, which may contribute to its analgesic properties *in vivo*.

List of non-standard abbreviations

AGE	advanced glycation end products
AWERB	Animal Welfare and Ethical Review Board
DAPI	4',6-diamidino-2-phenylindole
DRG	dorsal root ganglion/ganglia
FPSZM1	N-benzyl-4-chloro-N-cyclohexylbenzamide
HMGB1	high mobility group box-protein 1
PBS	phosphate buffered saline
PKC	protein kinase C
PVDF	polyvinylidene difluoride
RAGE	receptor for advanced glycation end products
rh	recombinant human
SDS-PAGE	sodium dodecyl sulphate- polyacrylamide gel electrophoresis
STZ	streptozotocin
TRP	transient receptor potential
VEGF-A	vascular endothelial growth factor-A

Diabetic neuropathy affects up to 50% of diabetic patients (Obrosova, 2009) and results from changes in the peripheral sensory nerve microenvironment due to microvasculopathy, and direct actions of high glucose on peripheral sensory neurons. Sensory neurons are particularly susceptible to hyperglycaemic damage as they lack insulin-regulated glucose uptake (Tomlinson and Gardiner, 2008). Peripheral sensory fibre damage in nerve trunks results in local inflammatory responses and the development of neuropathic pain including symptoms of allodynia and hyperalgesia in experimental and naturally occurring diabetes (Calcutt et al., 2008).

Long-standing hyperglycaemia results in the formation and accumulation of advanced glycation end products (AGEs) (Singh et al., 2014), which can activate the receptor for AGE (RAGE) and cause neuronal damage. Other RAGE ligands, such as the inflammatory cytokine high mobility group box-protein 1 (HMGB1, a.k.a. amphoterin), can act more rapidly to activate RAGE (Saleh et al., 2013), and may contribute to pain through modulation of neuro-inflammatory responses (Maeda et al., 2013). RAGE expression is increased in peripheral neurons in traumatic (Allette et al., 2014) and diabetic neuropathy (Juranek et al., 2013), and RAGE neutralisation inhibits neuropathic pain (Brederson et al., 2016). The mechanism(s) of RAGE signalling on sensory neuronal sensitisation are unknown.

HMGB1 levels are increased in plasma in diabetic patients (Devaraj et al., 2009) and HMGB1 is implicated in chronic pain (Agalave and Svensson, 2015) associated with arthritis (Ke et al., 2015), and traumatic (Allette et al., 2014; Feldman et al., 2012; Nakamura et al., 2013) and chemotherapy-induced neuropathic pain (Nishida et al., 2016), probably through RAGE activation (Allette et al., 2014). HMGB1 sensitises and activates sensory neurones in a manner that would lead to altered nociceptive behaviour (Feldman et al., 2012), but the mechanism through which these changes occur are unknown.

TRP channels such as TRPA1 and TRPV1 are implicated in both the pain (Cui et al., 2014; Pabbidi et al., 2008; Wei et al., 2009) and neuronal damage in diabetic neuropathy (Koivisto et al., 2012). The pain and neuronal damage in diabetic neuropathy are related to the decrease in expression of vascular endothelial growth factor-A (VEGF-A) (Jeric et al., 2017; Pawson et al., 2010), a family of growth factors with effects on both vascular and neuronal systems (Carmeliet and Storkebaum, 2002). We showed that pain and neuronal activation associated with one VEGF-A splice variant, VEGF-A_{165}a, are mediated through effects on TRPV1 (Hulse et al., 2014). These effects can be reversed by the alternatively spliced VEGF-A_{165}b isoform (Harper and Bates, 2008), which also decreases neuropathic pain behaviours in diabetic rats (Hulse et al., 2015).

In these studies we tested the hypotheses that:

1. Hyperglycaemia is associated with increased peripheral HMGB1 expression in diabetic rats when mechanical and thermal hypersensitivity is present;

2. HMGB1 sensitises neurons through actions on TRPV1;

3. High glucose conditions alter TRPV1-mediated signalling in sensory neurons through an HMGB1/RAGE/PKC-dependent mechanism, and

4. That the effects of HMGB1 on sensory neurons can be reversed by VEGF-A_{165}b treatment.

Results

STZ induced hyperglycaemia that, with low dose insulin treatment, was stable and sustained over at least 7 weeks, with little weight loss in the animals (Hulse et al., 2015). Weight loss was not observed in these animals over the 3 weeks of the study (see below). At three weeks animals showed significant thermal and mechanical hypersensitivity in the hind paws, which was ameliorated by systemic VEGF-A_{165}b treatment (Figure 1), consistent with published data (Hulse et al., 2015). As previously reported, VEGF-A_{165}b treatment had no effect on animal weight or blood glucose levels (Weights after 3 weeks of treatment: naives 289 ± 7 (mean±SEM), diabetes + vehicle 261 ± 6g, diabetes + VEGF-A_{165}b 264 ± 4g. Blood glucose levels: naives 6 ± 0.2mM/L, STZ + vehicle 27 ± 1nM/L, STZ + VEGF-A_{165}b 29 ± 0.8mM/L.

Animal weight and glucose levels at 7 weeks as previously published (Hulse et al., 2015)).

HMGB1 and RAGE expression is increased in STZ diabetic rats

HMGB1 protein expression was significantly increased in hind paw plantar skin at both 3 and 7 weeks post STZ injection. The change in expression of HMGB1 was not affected by treatment with VEGF-A_{165}b (Figure 1). We confirmed RAGE expression in dorsal root ganglion (DRG), which contains the cell bodies of somatosensory neurons (Figure 2A). RAGE expression was seen in the majority of DRG neurons, across the whole range of cell sizes, and changes in diabetes were not limited to a particular subgroup of neurons (data not shown). RAGE expression is in a positive feedback mechanism with RAGE activation and therefore we determined whether there was any change in RAGE expression in sensory neurons in diabetic rats. The proportion of DRG neurons positive for RAGE expression was increased in diabetic rats compared to naïve, as previously reported (Zochodne, 2014), and this was unaffected by VEGF-A_{165}b treatment (Figure 2B). The intensity of the RAGE staining in individual RAGE positive DRG neurons was also increased in diabetic rats compared to naïve, and this increase was partially ameliorated by VEGF-A_{165}b (Figure 2).

Enhanced TRPV1-evoked calcium responses in STZ diabetic rats DRG neurons is a hyperglycaemia-mediated event and is prevented by VEGF-A_{165}b treatment.

TRPV1 contributes to primary sensory neuronal sensitisation in many pain states (Marwaha et al., 2016), including diabetes (Cui et al., 2014; Pabbidi et al., 2008), and the degree of behavioural hypersensitivity is associated with increased agonist-evoked TRPV1 activity. We therefore determined whether DRG neurons isolated from diabetic rats showed increased TRPV1 agonist-evoked calcium responses. Capsaicin evoked a larger response in DRG neurons from female diabetic rats compared to DRG neurons from naïve female rats (Figure 3A). This effect could be modelled in DRG neurons from adult naïve male rats exposed to 24h of high glucose (50mM glucose), with an increased intracellular calcium fluorescence response to 1µM capsaicin compared to basal glucose conditions (Figure 3B). This demonstrates that the enhanced TRPV1-evoked calcium responses were, at least in part, a hyperglycaemia-induced effect. The inclusion of equimolar mannitol in the basal glucose condition indicates that effects of 50mM glucose cannot be attributed to any osmotic effect of the additional glucose. The specific TRPV1 antagonist capsazepine blocked the capsaicin (Cap)-evoked change in intracellular calcium in primary sensory neurons in this assay, in a concentration-dependent manner (Figure 3C), with an IC_{50} of ~1µM.

High glucose-mediated increased TRPV1-evoked calcium responses were significantly reduced when DRG neurons were co-treated with VEGF-A_{165}b in high glucose conditions (Figure 4). TRPV1 sensitisation, which leads to increased calcium influx, has previously been attributed to increased phosphorylation, particularly at serine 800 (Mandadi et al., 2006; Wang et al., 2015), which is a PKC-dependent phosphorylation site. In immortalised embryonic rodent DRG neurons (50B11) exposed to high glucose conditions phosphorylation of TRPV1 at S800 increased compared to basal glucose conditions, with no effect on total TRPV1 expression ((Radu et al., 2013), see also (Khomula et al., 2013; Mohammadi-Farani et al., 2014)). Both high-glucose-enhanced TRPV1 calcium responses (Figure 4A, B) and TRPV1 phosphorylation (Figure 4C-D) were reduced after 24h exposure to VEGF-A_{165}b, even though TRPV1 expression was slightly increased by VEGF-A_{165}b treatment (Figure 4E).

Increased RAGE activity contributes to high glucose-induced TRPV1-evoked calcium responses in DRG neurons

As the RAGE agonist HMGB1 was increased in the skin (i.e. in the tissues surrounding nociceptive neuronal terminals) of diabetic animals, we hypothesised that the altered neuronal sensitivity to TRPV1 agonists seen *in vitro* could be RAGE-dependent. The RAGE antagonist FPSZM1 did not affect capsaicin-evoked TRPV1 calcium changes in normal glucose concentrations (Figure 5A), but reduced calcium fluorescence in high glucose conditions in a concentration-dependent manner (Figure 5B). Concentrations

of FPSZM1 above 10nM reduced capsaicin-evoked calcium responses to control levels (Figure 5C).

HMGB1 increases TRPV1-agonist-evoked calcium responses, and is a RAGE mediated effect that is blocked with VEGF-A_{165}b

HMGB1 is a RAGE agonist that has been implicated in peripheral nociceptive signalling (Feldman et al., 2012). HMGB1 increased capsaicin-evoked TRPV1 calcium responses in DRG neurons (10mM glucose; Figure 5D) and this was reduced by incubation with 10nM FPSZM1 (Figure 5E). Inhibition of PKC activity by incubation of DRG neurons with HMGB1 and 1µM BIM-1 reduced capsaicin-evoked TRPV1 calcium changes (Figure 6A). HMGB1-enhanced TRPV1-evoked calcium responses were also reduced following 24h treatment with VEGF-A_{165}b (Figure 6B).

Effect sizes for data in all experiments are shown in Table S1.

Discussion

These data collectively show for the first time that, *in vitro*, 1) high glucose concentrations alter TRPV1-evoked calcium responses in DRG neurons through RAGE; 2) HMGB1 alters TRPV1-evoked calcium responses through RAGE in DRG neurons under basal glucose conditions, which is PKC dependent, and blocked by VEGF-A_{165}b, and 3) HMGB1 is up-regulated in skin in diabetic rats. This is the first study to demonstrate a potential neuronal mechanism through which HMBG-1/RAGE could alter DRG neuronal properties under high glucose conditions *in vitro*.

There have been many proposed causes for painful diabetic neuropathy. These include microvasculopathic neuronal hypoxia, direct effects of glucose toxicity on sensory neurons, and activation of TRPA1 and other ion channels in sensory neurons by reactive metabolites such as methylglyoxal (Andersson et al., 2013; Huang et al., 2016). In the later stages of the condition, RAGE activation by AGEs is driven by molecules such as methylglyoxal, resulting in cellular damage, and further complications (Hidmark et al., 2014). RAGE is a pattern recognition receptor that is capable of signalling local tissue damage (Kato et al., 2016). Activation of RAGE by AGEs usually results after significant accumulation of AGEs over time (months to years *in vivo*), and is considered to be a late contributor to diabetic complications (Singh et al., 2014). Herein we show that neuronal RAGE activity in sensory neurons is not detectable in neurons cultured in normal glucose concentrations, but is

evident following a short (24h) exposure to high glucose (50mM) *in vitro*. AGE formation is reported to occur after 6-10 days in 2M glucose *in vitro* (Hori et al., 2012), suggesting that our experimental conditions would not be sufficient to cause AGE generation. Thus, we hypothesise that neuronal RAGE activation after short exposure to high glucose, possibly through the more rapid generation of HMGB1, could contribute to early changes in neuronal properties, resulting in enhanced nociception.

Importantly the endogenous RAGE agonist HMGB1 itself alters TRPV1-evoked neuronal responses under normal glucose conditions. HMBG1 has been found in Schwann cells, DRG satellite cells and primary sensory neurons in traumatic neuropathy (Wan et al., 2016), in sensory neurons in experimental diabetes (Juranek et al., 2013), and human diabetic nerve (Bierhaus et al., 2004). HMGB1 has been implicated in peripheral mechanisms of pain through both direct (Allette et al., 2014) and indirect activation of sensory neurons through interaction with pro-inflammatory molecules such as IL-1 and TNFα (Wan et al., 2016), and RAGE-mediated pro-inflammatory cytokine release from immune cells (Kato et al., 2016). Taken together, our data support a direct effect of HMGB1 on sensory neurons, with rapid (≤24h) onset, that can be induced under high glucose conditions *in vitro*, extending our understanding of the function of HMGB1 and its effects on functional neuronal change. As the RAGE agonist HMGB1 is increased in skin in diabetic rats when pain behaviour is altered (data herein (Hulse et al., 2015)), and RAGE expression is increased in sensory neurons (Zochodne, 2014), these peripheral actions of HMGB1 may be a contributory

factor in the pain associated with glucose-induced neuronal damage and pain in diabetes.

Modulation of the TRP channels TRPA1 and TRPV1 has been implicated in both neuronal damage and pain in diabetic neuropathy (Cui et al., 2014; Hong and Wiley, 2005; Khomula et al., 2013). TRPA1 and TRPV1 are important molecules in the sensitisation of peripheral nociceptive afferents (Cheng and Ji, 2008), and TRPV1 is directly sensitised by high glucose conditions in sensory neurons (Lam et al., 2018) and in diabetes *in vivo* (Hong and Wiley, 2005; Khomula et al., 2013). TRPV1 phosphorylation by PKC at serine-800 is key to its sensitisation (Wang et al., 2015). Both S800-TRPV1 phosphorylation and sensitisation can be increased in high glucose conditions *in vitro*, and by RAGE activation by HMGB1. TRPV1 is phosphorylated and sensitised by a PKC-dependent mechanism in diabetes *in vivo* (Hong and Wiley, 2005). RAGE-PKC interactions can also modulate neuronal function *in vivo*, affecting conduction velocity slowing (indicative of peripheral neuronal damage), as well as neuronal repair in diabetic neuropathy (Zochodne, 2014). While other signalling pathways, such as PKA, are also known to contribute to sensory neuronal sensitisation (Cheng and Ji, 2008), our data are consistent with PKC-mediated phosphorylation of sensory neuronal TRPV1 being one important mechanism through which HMGB1, and presumably other RAGE agonists, could rapidly sensitise peripheral neurons. This could contribute to pain in conditions where HMGB-1 is expressed, such as various neuropathic conditions (Allette et al., 2014; Brederson et al., 2016; Juranek et al., 2013).

While TRPV1 expression changes were reported in specific DRG neuronal subpopulations, total TRPV1 levels were reported to *decrease* in DRG in diabetic rats (Hong and Wiley, 2005). Despite this overall decrease in TRPV1 expression, neuronal TRPV1 functional responses were increased (sensitised) through a PKC-dependent mechanism (Hong and Wiley, 2005). This agrees with our findings under high glucose conditions *in vitro* and suggests that our reported differences between naïve and diabetic DRG calcium responses *ex vivo* are not attributable to alteration in TRPV1 expression levels alone. We found no change in neuronal TRPV1 expression in high glucose conditions (Fig. 4). It should also be noted that in measuring intracellular calcium levels, albeit evoked by a TRPV1 agonist, the enhanced responses we report might represent TRPV1 sensitisation *in vitro* and *ex vivo*, but could also be attributable to changes in other ion channels. RAGE can directly contribute to PKC-dependent capsaicin-induced non-TRPV1-mediated intracellular calcium increases in high glucose conditions (Lam et al., 2018). TRPA1 is also sensitised in rat DRG immortalised neurons (50B11) in high glucose conditions *in vitro* (Hulse et al., 2015) and in animal models of diabetes. TRPA1 forms complexes with TRPV1, and can affect TRPV1 function, such as reducing desensitisation, thus potentially altering calcium responses (Masuoka et al., 2017; Staruschenko et al., 2010). There is, however, no evidence that RAGE can directly alter TRPA1 function. Voltage-gated sodium and calcium channels are also involved in diabetic pain in STZ rodents, for example through methylglyoxal-RAGE-mediated effects on Nav1.8 (Huang et al., 2016), TNF-α/NFκB-mediated upregulation of Nav1.7 (Huang et al., 2014), or upregulation of calcium channel subunits (Yusaf et al.,

2001). All of these effects will contribute to the known changes in nociceptor properties in diabetes *in vivo* (Chen and Levine, 2001), and could also contribute to the *in vitro* changes that we report.

Hypoxia, known to affect peripheral tissues including nerves, is a potent stimulus for TRPV1 sensitisation through hypoxia-inducible factor (HIF) -1 alpha and PKC (Ristoiu et al., 2011). Hypoxia and HIF-1α also induce expression of the pro-nociceptive VEGF-A isoform VEGF-A_{165}a, which also sensitises TRPV1 through PKC (Hulse et al., 2014). We have previously shown that bi-weekly treatment with rhVEGF-A_{165}b reverses both pain and neuronal terminal loss in experimental diabetes, and sensitisation of sensory neuronal TRPA1-evoked responses (Hulse et al., 2015). Given that RAGE expression is up-regulated by HMGB1, the reduction in RAGE intensity *in vivo* by VEGF-A_{165}b treatment (Fig. 3C) suggests that this treatment could reduce HMGB1 activation of RAGE, or modify the downstream signalling from HMGB1/RAGE activation that results in the feed-forward agonist-induced up-regulation of RAGE, resulting in reduced pain, rather than exerting direct effects on neuronal TRPV1. This requires confirmation, as does the contribution of HMGB1/RAGE/TRPV1 to altered pain behaviour in diabetic neuropathy *in vivo*. Blockade of HMGB1/RAGE-mediated neuronal sensitisation by rhVEGF-A_{165}b *in vitro* supports our hypothesis that alteration of VEGF-A isoforms, for example by treatment with rhVEGF-A_{165}b or an agent that alters VEGF-A splicing to favour VEGF-A_{165}b may be an effective treatment for diabetic neuropathy.

Materials and methods

Cell culture reagents (media and media supplements) and equipment were supplied by Invitrogen Life Technologies (Paisley, UK). Protein extraction buffer, supplements, buffers, and solutions, streptozotocin and sodium pentobarbital were supplied by Sigma-Aldrich (Irvine, UK) and Western blot reagents and equipment through Bio-Rad (CA, USA). Superfrost plus slides and OCT embedding medium were supplied by VWR International, (PA, USA) and DAPI by Vector laboratories, (Peterborough, UK). Behavioural testing equipment was supplied by Ugo Basile (Varese Italy).
Drugs were supplied by R&D Systems (MA, USA) (rhVEGF-A_{165}b and rhHMGB1), EMD Millipore (MA, USA) (FPSZM1) and LinShin (insulin pellets). Details of antibodies and sources are shown in Table 1.

A total of 63 male and female rats (Charles River Laboratories, Kent, UK) were used in this study. All experiments were carried out in laboratories at the University of Nottingham in accordance with the EU 2010/63 Directive, the United Kingdom's Scientific Procedures Act 1986 and associated amendments and guidelines (2012) and were approved by the University of Nottingham AWERB (Animal Welfare and Ethical Review Board). The experiments in these studies conformed to the principles of the ARRIVE guidelines. Animals were housed at 21ºC and 55% relative humidity with a 12h light-dark cycle. For diabetic animals food and water were provided *ad libitum* except immediately prior to STZ injection.

Humane endpoints included loss of body weight >15%; animal behaviour indicative of pain or distress, such as staring coat, immobility, hunched stance (no animals met any of these endpoints). All rats were group housed (minimum 2 animals per cage) under 12 hour light-dark cycles, with additional paper bedding material and environmental enrichment, *ad libitum* access to standard chow and water. Due to increased urination in diabetic animals, bedding and cage materials were changed frequently, usually at need rather than at specific time intervals.

Adult female Sprague Dawley rats (~250g, n=35) were used in the *in vivo* diabetes study. Adult female Sprague Dawley rats were used for STZ-diabetes as these animals reach the top of their growth curve at about this age. It is therefore easier to monitor animal welfare, as even small amounts of weight loss in comparison to untreated control animals is evident with correction for any growth-related weight gain (Calcutt, 2004). Adult male Wistar rats (~250-350g, n=29) were used for primary dorsal root ganglion neuronal cultures *in vitro*, as previously reported (Hulse et al., 2014; Hulse et al., 2015).

Animal numbers were determined *a priori* based on effect sizes in multiple measures derived from a previous group of animals that underwent the same procedures in a previous study using G*Power (Faul et al., 2007; Hulse et al., 2015)

Diabetes was induced with an intraperitoneal injection (i.p.) of streptozotocin (STZ; 50mg.kg^{-1}) as previously described (Hulse et al., 2015). Hyperglycaemia (>15mM circulating glucose) was confirmed 4 days after STZ injection; in animals in which hyperglycaemia was not confirmed after initial STZ injection, a second STZ injection was administered. Animals in which STZ injection did not result in hyperglycaemia (n=6) were not used in further experiments. STZ-injected hyperglycaemic animals were treated with very low dose insulin supplementation with 1/3 of a LinShin insulin pellet injected subcutaneously in the scruff of the neck under brief general isofluorane anaesthesia (2-3% in O_2), and using the sterile trocar supplied by the manufacturer (Calcutt, 2004; Hulse et al., 2015). Animals were supplied with concentrated sucrose solution to reduce the incidence of hypoglycaemia in the 24h immediately post-STZ injection (Calcutt, 2004). Experimental groups were: diabetic rats treated bi-weekly with recombinant human (rh)VEGF-A_{165}b injection (20ng.g^{-1} body weight, n=9) or phosphate buffered saline (PBS, VEGF vehicle, n=9) (Hulse et al., 2015). Age matched naïve rats (n=11) served as non-diabetic controls. Bi-weekly injections of VEGF-A_{165}b and PBS began 1 week after confirmation of both hyperglycaemia and altered nociceptive behaviour, a treatment regime we have previously shown to be effective in traumatic and diabetic neuropathies (Hulse et al., 2014; Hulse et al., 2015). Animals were maintained for a further 3 weeks after confirmation of hyperglycaemia. Weekly thermal and mechanical nociceptive testing was performed throughout the duration of the study.

Rats were habituated to nociceptive behavioural testing environments for 2 weeks prior to STZ injection and for 20 minutes before the start of each weekly session. Thermal nociceptive testing was performed using the Hargreaves test (Hargreaves et al., 1988). The intensity of the radiant heat source was set so that the mean response latency was ~10s in naïve animals at baseline testing and the intensity was kept constant throughout the duration of the study. Three latencies were measured in each testing session and the mean value calculated. To prevent heat induced tissue damage an inter-stimulus interval of a minimum of 5 minutes was used between measurements. Mechanical nociceptive testing was performed using von (v)Frey monofilaments as previously described (Hulse et al., 2014; Hulse et al., 2015). vFrey monofilaments of varying force were applied to the plantar surface of the hind paw 5 times each to generate a stimulus-response curve and the withdrawal threshold (force in grams) was calculated as the force at which the animal withdrew to 50% of stimulus presentations. For both thermal and mechanical testing, measurements were taken for both left and right hind paws and the data were treated as duplicates for each animal. The animal was taken as the independent observation not the paw. The operator performing behavioural testing was blinded to the treatment groups as another researcher coded the injections for treatments. As the operator administering the injections was blinded, this resulted in a randomisation of treatment order.

After 3 weeks, rats were terminally anesthetized (sodium pentobarbital 60mg.kg^{-1}, i.p.) and transcardially perfused with PBS. Plantar skin and L3/4/5 DRG were dissected and a) immediately snap frozen on dry ice and then transferred to -80°C before processing for protein extraction or b) DRG were dissected and post-fixed for 24h in 4% paraformaldehyde (PFA, pH 7.4) at 4°C and then transferred to 30% sucrose solution for a further 24 h at 4°C for immunofluorescence.

***In vitro* assessment of TRPV1 expression and phosphorylation.**

50B11 neurons (a gift from Ahmed Hoke, provided through Damon Lowes, see Acknowledgements) are an immortalized dorsal root ganglion sensory neuronal cell line derived from embryonic rats (Chen et al., 2007) and were used as a model system to determine changes in total TRPV1 and phosphorylated TRPV1 under different glucose conditions, and to reduce the numbers of animal numbers used. These cells were authenticated in house as expressing functional neuronal markers, particularly those associated with nociception such as TRPA1 and TRPV1(Bestall, 2017). 50B11s were maintained in neurobasal media supplemented with 10% foetal bovine serum, 0.55mM glutamine, B27 supplement and an additional 11mM glucose (making the total glucose concentration 36mM (Chen et al., 2007)). Basal glucose concentration is thus higher for 50B11 maintenance than for primary sensory neurons, but is required for their culture. 50B11 neurons have impaired neurite outgrowth in both normal (5mM) and high (66mM) glucose conditions (Bestall, 2017).

50B11 neurons were differentiated for 24h with 1nM nerve growth factor (NGF) and 75µM forskolin and then treated for a further 24h under the following conditions: basal glucose (36mM glucose + 30mM mannitol), high glucose (66mM glucose) ± recombinant human VEGF-A_{165}b (2.5nM) or PBS (VEGF vehicle). After 24h, protein was extracted and subject to Western blotting for TRPV1 and phospho-serine 800-(p800)TRPV1. Equimolar mannitol addition controlled for any potential effect of increased osmolarity under high glucose conditions.

Western blotting.

Protein was extracted in RIPA buffer containing 150mM sodium chloride, 1% nonyl phenoxypolyethoxylethanol (NP-40), 0.5% sodium deoxycholate, 0.1% SDS, and 50mM Tris (pH 8.0) supplemented with protease inhibitor cocktail (20µl.ml^{-1} buffer; 1mM phenylmethylsulfonyl fluoride, 10mM sodium orthovanadate and 50mM sodium fluoride). Equal amounts of protein were loaded and separated on a 4-20% gradient precast SDS-PAGE gel and proteins transferred to a PVDF membrane using wet transfer. Membranes were incubated in blocking buffer (5% bovine serum album in Tris buffered saline containing 0.1% Tween 20) for 60 minutes at room temperature and incubated overnight at 4°C in primary antibodies against TRPV1, p800-TRPV1, and HMGB1 (Table 1) diluted in blocking solution. Loading was confirmed and differences determined by concurrent probing for actin expression. Membranes were then washed in PBS and fluorescent secondary antibodies (Table 1) were applied in blocking solution for 60 minutes at room

temperature. Membrane fluorescence was visualized and analysed on a Licor Odyssey Fc.

Immunofluorescence

Following fixation and cryoprotection of tissue from diabetic rats, DRG were embedded and frozen at -80°C before sectioning at 8µm thickness. Sections were then stored mounted on slides (Superfrost plus) at -80°C. Sections were washed in PBS, blocked with 5% bovine serum albumin, 10% foetal bovine serum in PBS + 0.2% Triton X-100). Sections were incubated in primary antibodies against RAGE and NeuN (Table 1) in blocking solution overnight at 4°C. Slides were washed in PBS and incubated in fluorescent secondary antibodies in PBS-0.2% Triton X100 for 2 h at room temperature, then coverslipped with Vectorshield mounting media containing DAPI (4',6-diamidino-2-phenylindole). A minimum of 5 randomly selected non-serial images were acquired from at least 5 sections from each animal per treatment group at 20x magnification using consistent microscope settings between channels on a Leica TCS SPE confocal microscope and the Leica applications suite software (LAS X). All immunofluorescence images were equally enhanced (30% increase in brightness, 0% change in contrast) for presentation (Figure 3). Images were exported for further analysis in Image J software (specifically FIJI)(Schindelin et al., 2012). The number of RAGE positive neurons was determined by counting the number of NeuN positive DRG neurons that co-expressed RAGE. RAGE intensity analysis was performed using the mean grey area values for these neurons. For each image containing RAGE positive neurons, a local mean grey area background

value was subtracted from experimental values. All image analysis was performed blinded to treatment group on raw images. The images shown (Figure 2) are altered for brightness (+35%) and contrast (-20%) compared to the raw images used for analysis. The RAGE antibody (Table 1) detected a single band of ~45kD as expected, in 50B11 neurons (Figure S1).

TRPV1 activity *in vitro*.

For primary sensory neuronal culture, widely used to study mechanisms of neuronal signalling and sensitisation using single cell approaches (Huang et al., 2015) through to high throughput screening (Hulse et al., 2014; Newberry et al., 2016), adult male Wistar rats were killed by anaesthetic overdose (60mgkg^{-1} sodium pentobarbital, i.p. injection) and death verified by confirmation of cessation of the circulation.

T1-L6 DRGs were dissected, enzymatically and mechanically dissociated, and cultured on poly-L-lysine/ laminin coated 96 well plates (black sided, Costar) at a seeding density of 2000 cells per well in Ham's F12 medium containing 1x N2 supplement 1% BSA and 1% penicillin streptomycin. Equal numbers of cells were seeded per well to reduce the inter- and intra-assay variability between wells. After cell attachment, cultures were treated with 30µg.ml^{-1} 5-fluoro-2'-deoxyuridine to prevent mitosis of non-neuronal cells. Neuronal cultures were maintained in basal glucose conditions (10mM glucose +40mM mannitol as an osmotic control) or high glucose conditions (50mM glucose) for 24h +/- the following co- treatments: 2.5nM rhVEGF-A_{165}b; rhHMGB1 (1-100nM); FPSZM1 (RAGE antagonist 1-100nM), and 1µM BIM-1 (PKC inhibitor). Cells were then loaded with Fluo-4 (Invitrogen) in

Hank's balanced buffered saline solution containing 20mM HEPES and 2mM $CaCl_2$ for 1 hour. The TRPV1 agonist capsaicin (1µM unless otherwise stated, concentration chosen based on previous findings (Hulse et al., 2014) known to be in the range for agonist-specific TRPV1-evoked responses (Edwards, 2014)) was used to stimulate TRPV1 channels and the resulting changes in intracellular calcium fluorescence were measured on a Victor X4 plate reader at 37°C over a 160 second period. In some experiments, to verify the calcium response as being evoked through activation of TRPV1, primary neuronal cultures were dissociated, plated and maintained in basal glucose for 24 h. Following loading with Fluo-4, capsazepine or vehicle (0.03% DMSO) was added to the culture 20 minutes prior to addition of 1µM capsaicin and calcium assay. In all assays baseline readings were determined prior to initial capsaicin application and under control conditions to determine any background signal. The sequential fluorescence recordings were corrected for background, and expressed as a fold change of respective baseline values to reduce inter-well variance and to control for minor variations in cell number (Hulse et al., 2014). The inter-assay mean coefficient of variation was 8.9% (from n=11 independent experiments, each containing 3-20 repeats all performed by SMB). Fluorometric imaging plate assays such as this are widely used to assay TRPV1 responses to capsaicin in transfected and native cells; responses are known to be TRPV1-dependent (Gunthorpe et al., 2007; Pineau et al., 1996; Rami et al., 2006; Tafesse et al., 2004; Wang et al., 2014; Zhuang et al., 2004). Each plate contained DRG neurons from a single rat and in each replicate plate cells were exposed to the same combination of experimental treatment conditions in a block design, to allow comparison of

responses within and between plates. For reproducibility each assay was performed multiple times as noted in the text, and each independent plate was exposed to identical treatments in each experiment. Calcium levels were normalised to baseline measures in each plate to allow for pooling of data derived from replicates, as is usual with repeated high throughput assays (Iversen et al., 2004).

This assay uses TRPV1 as a read-out for altered nociceptive neuronal activity, and thus these experiments were not designed to investigate precise mechanisms of TRPV1 modulation. We have previously validated this high-throughput assay for its ability to replicate the effects of compounds assayed by single cell patch clamp analysis (Hulse et al., 2014). The use and comparison of capsaicin-evoked calcium responses in each assay limits the comparisons being made to the responses of the TRPV1-expressing nociceptive population of sensory neurons in the rat, ensuring comparison of like responses between assays. The TRPV1-expressing population represents ~65% of DRG nociceptors (peptidergic + $IB4^+$ populations (Price and Flores, 2007).

Experimental design, data extraction and analysis

Effect sizes and representative data values for experiments in this manuscript are given in the Supplementary Information (Table S1). TRPV1 activity assay sample size calculations were determined using previously published data (Hulse et al., 2014; Hulse et al., 2015) and the following parameters: repeated measures ANOVA, between factor, power 0.8, number of groups 3, number of measurements per group, 21. Sample size calculation for behavioural

experiments was based on a two tailed non-parametric analysis (Mann Whitney), minimum required power 0.8. Numbers of animals used were calculated to give sufficient power for further tissue analyses on subgroups given the possibility for tissue loss and small tissue samples (DRG).

All data are presented as mean ±SEM and *n* values given represent independent observations, which are usually individual animals or independent cultures/treatments. Multiple group comparisons were made by one-way ANOVA (treatment effects), Kruskal-Wallis (KW, treatment effects) or two-way ANOVA (treatment effects over time, or with agonist concentration), all two tailed tests, as stated in Figure legends. Overall effects of different condition effects on neuronal calcium over time were compared by comparison of integrated area under the curve for each independent assay followed by comparison using parametric/non-parametric ANOVA as stated in Figure legends. For concentration:response curves (Figures 4 & 6), each individual data point comprises of the mean AUC, rather than peak calcium response, from the stated number of experimental repeats. Pair wise post-hoc comparisons were made using Sidak's tests or Dunn's tests as stated in Figure legends, with correction for multiple comparisons, when ANOVA significance was reached. Alpha was set at 0.05. All statistical analysis was performed using GraphPad Prism v6-7 for Windows and Mac, (GraphPad Software, La Jolla California USA, www.graphpad.com).

Acknowledgements

We thank Ahmet Hoke, John's Hopkins University, and Damon Lowes, University of Aberdeen for the gift of the 50B11 cell line.

Funding

This work was supported by funding from the University of Nottingham (SMB, RPH, DOB, LFD), Diabetes UK (11/0004192 to LFD, and 10/0004152 to DOB), The Medical Research Council UK (MR/K020366/1 to DOB), the Richard Bright VEGF Research Trust (UK Registered Charity 1095785), the European Foundation for the Study of Diabetes Microvascular Programme supported by Novartis (to RPH) and Arthritis Research UK (20400 to LFD, RPH & DOB).

Competing interests

LFD and DOB are co-inventors on patents protecting alternative RNA splicing control and VEGF-A splice variants for therapeutic application in a number of different conditions. LFD and DOB are founder equity holders in, and consultants (both) and director (DOB) to Exonate Ltd, a University of Nottingham spin-out company with a focus on development of alternative RNA splicing control for therapeutic application in a number of different conditions, including analgesia and neuroprotection (www.exonate.com). Exonate made no financial contribution to this study. The University of Nottingham also holds equity in Exonate Ltd.

References

Agalave, N. M. and Svensson, C. I. (2015). Extracellular high-mobility group box 1 protein (HMGB1) as a mediator of persistent pain. *Mol Med* **20**, 569-78.

Allette, Y. M., Due, M. R., Wilson, S. M., Feldman, P., Ripsch, M. S., Khanna, R. and White, F. A. (2014). Identification of a functional interaction of HMGB1 with Receptor for Advanced Glycation End-products in a model of neuropathic pain. *Brain Behav Immun* **42**, 169-77.

Andersson, D. A., Gentry, C., Light, E., Vastani, N., Vallortigara, J., Bierhaus, A., Fleming, T. and Bevan, S. (2013). Methylglyoxal evokes pain by stimulating TRPA1. *PLoS One* **8**, e77986.

Bestall, S. M. (2017). Diabetic neuropathy: A mechanism of TRPV1 sensitisation and the treatment with Vascular Endothelial Growth Factor-A165b (VEGF-A165b). In *School of Life Sciences*, vol. PhD, pp. 225. Nottingham, UK: University of Nottingham.

Bierhaus, A., Haslbeck, K. M., Humpert, P. M., Liliensiek, B., Dehmer, T., Morcos, M., Sayed, A. A., Andrassy, M., Schiekofer, S., Schneider, J. G. et al. (2004). Loss of pain perception in diabetes is dependent on a receptor of the immunoglobulin superfamily. *J Clin Invest* **114**, 1741-51.

Brederson, J. D., Strakhova, M., Mills, C., Barlow, E., Meyer, A., Nimmrich, V., Leddy, M., Simler, G., Schmidt, M., Jarvis, M. et al. (2016). A monoclonal antibody against the receptor for advanced glycation end products attenuates inflammatory and neuropathic pain in the mouse. *Eur J Pain* **20**, 607-14.

Calcutt, N. A. (2004). Modeling Diabetic Sensory Neuropathy in Rats. In *Pain Research: Methods and Protocols*, vol. 99 (ed. Z. D. Luo), pp. 55-65: Springer.

Calcutt, N. A., Jolivalt, C. G. and Fernyhough, P. (2008). Growth factors as therapeutics for diabetic neuropathy. *Curr Drug Targets* **9**, 47-59.

Carmeliet, P. and Storkebaum, E. (2002). Vascular and neuronal effects of VEGF in the nervous system: implications for neurological disorders. *Semin Cell Dev Biol* **13**, 39-53.

Chen, W., Mi, R., Haughey, N., Oz, M. and Hoke, A. (2007). Immortalization and characterization of a nociceptive dorsal root ganglion sensory neuronal line. *J Peripher Nerv Syst* **12**, 121-30.

Chen, X. and Levine, J. D. (2001). Hyper-responsivity in a subset of C-fiber nociceptors in a model of painful diabetic neuropathy in the rat. *Neuroscience* **102**, 185-92.

Cheng, J. K. and Ji, R. R. (2008). Intracellular signaling in primary sensory neurons and persistent pain. *Neurochem Res* **33**, 1970-8.

Cui, Y. Y., Xu, H., Wu, H. H., Qi, J., Shi, J. and Li, Y. Q. (2014). Spatio-temporal expression and functional involvement of transient receptor potential vanilloid 1 in diabetic mechanical allodynia in rats. *PLoS One* **9**, e102052.

Del Nagro, C. J., Choi, J., Xiao, Y., Rangell, L., Mohan, S., Pandita, A., Zha, J., Jackson, P. K. and O'Brien, T. (2014). Chk1 inhibition in p53-

deficient cell lines drives rapid chromosome fragmentation followed by caspase-independent cell death. *Cell Cycle* **13**, 303-14.

Devaraj, S., Dasu, M. R., Park, S. H. and Jialal, I. (2009). Increased levels of ligands of Toll-like receptors 2 and 4 in type 1 diabetes. *Diabetologia* **52**, 1665-8.

Edwards, J. G. (2014). TRPV1 in the central nervous system: synaptic plasticity, function, and pharmacological implications. . In *Capsaicin as a therapeutic molecule*, (ed. O. M. E. Abdel-Salam), pp. 86: Springer.

Faul, F., Erdfelder, E., Lang, A. G. and Buchner, A. (2007). G*Power 3: a flexible statistical power analysis program for the social, behavioral, and biomedical sciences. *Behav Res Methods* **39**, 175-91.

Feldman, P., Due, M. R., Ripsch, M. S., Khanna, R. and White, F. A. (2012). The persistent release of HMGB1 contributes to tactile hyperalgesia in a rodent model of neuropathic pain. *J Neuroinflammation* **9**, 180.

Genead, R., Fischer, H., Hussain, A., Jaksch, M., Andersson, A. B., Ljung, K., Bulatovic, I., Franco-Cereceda, A., Elsheikh, E., Corbascio, M. et al. (2012). Ischemia-reperfusion injury and pregnancy initiate time-dependent and robust signs of up-regulation of cardiac progenitor cells. *PLoS ONE* **7**, e36804.

Gunthorpe, M. J., Hannan, S. L., Smart, D., Jerman, J. C., Arpino, S., Smith, G. D., Brough, S., Wright, J., Egerton, J., Lappin, S. C. et al. (2007). Characterization of SB-705498, a potent and selective vanilloid receptor-1 (VR1/TRPV1) antagonist that inhibits the capsaicin-, acid-, and heat-mediated activation of the receptor. *J Pharmacol Exp Ther* **321**, 1183-92.

Hargreaves, K., Dubner, R., Brown, F., Flores, C. and Joris, J. (1988). A new and sensitive method for measuring thermal nociception in cutaneous hyperalgesia. *Pain* **32**, 77-88.

Harper, S. J. and Bates, D. O. (2008). VEGF-A splicing: the key to anti-angiogenic therapeutics? *Nat Rev Cancer* **8**, 880-7.

Hidmark, A., Fleming, T., Vittas, S., Mendler, M., Deshpande, D., Groener, J. B., Muller, B. P., Reeh, P. W., Sauer, S. K., Pham, M. et al. (2014). A new paradigm to understand and treat diabetic neuropathy. *Exp Clin Endocrinol Diabetes* **122**, 201-7.

Hong, S. and Wiley, J. W. (2005). Early painful diabetic neuropathy is associated with differential changes in the expression and function of vanilloid receptor 1. *J Biol Chem* **280**, 618-27.

Hori, M., Yagi, M., Nomoto, K., Ichijo, R., Shimode, A., Kitano, T. and Yonei, Y. (2012). Experimental Models for Advanced Glycation End Product Formation Using Albumin, Collagen, Elastin, Keratin and Proteoglycan. *Anti-ageing Medicine* **9**, 125-134.

Huang, D., Huang, S., Peers, C., Du, X., Zhang, H. and Gamper, N. (2015). GABAB receptors inhibit low-voltage activated and high-voltage activated Ca(2+) channels in sensory neurons via distinct mechanisms. *Biochem Biophys Res Commun* **465**, 188-93.

Huang, Q., Chen, Y., Gong, N. and Wang, Y. X. (2016). Methylglyoxal mediates streptozotocin-induced diabetic neuropathic pain via activation of the peripheral TRPA1 and Nav1.8 channels. *Metabolism* **65**, 463-74.

Huang, Y., Zang, Y., Zhou, L., Gui, W., Liu, X. and Zhong, Y. (2014). The role of TNF-alpha/NF-kappa B pathway on the up-regulation of voltage-

gated sodium channel Nav1.7 in DRG neurons of rats with diabetic neuropathy. *Neurochem Int* **75**, 112-9.

Hulse, R. P., Beazley-Long, N., Hua, J., Kennedy, H., Prager, J., Bevan, H., Qiu, Y., Fernandes, E. S., Gammons, M. V., Ballmer-Hofer, K. et al. (2014). Regulation of alternative VEGF-A mRNA splicing is a therapeutic target for analgesia. *Neurobiol Dis* **71**, 245-59.

Hulse, R. P., Beazley-Long, N., Ved, N., Bestall, S. M., Riaz, H., Singhal, P., Ballmer Hofer, K., Harper, S. J., Bates, D. O. and Donaldson, L. F. (2015). Vascular endothelial growth factor-A165b prevents diabetic neuropathic pain and sensory neuronal degeneration. *Clin Sci (Lond)* **129**, 741-56.

Iversen, P. W., Beck, B., Chen, Y. F., Dere, W., Devanarayan, V., Eastwood, B. J., Farmen, M. W., Iturria, S. J., Montrose, C., Moore, R. A. et al. (2004). HTS Assay Validation. In *Assay Guidance Manual*, (eds G. S. Sittampalam N. P. Coussens K. Brimacombe A. Grossman M. Arkin D. Auld C. Austin J. Baell B. Bejcek T. D. Y. Chung et al.). Bethesda (MD).

Jeric, M., Vukojevic, K., Vuica, A. and Filipovic, N. (2017). Diabetes mellitus influences the expression of NPY and VEGF in neurons of rat trigeminal ganglion. *Neuropeptides* **62**, 57-64.

Juranek, J. K., Kothary, P., Mehra, A., Hays, A., Brannagan, T. H., 3rd and Schmidt, A. M. (2013). Increased expression of the receptor for advanced glycation end-products in human peripheral neuropathies. *Brain Behav* **3**, 701-9.

Kato, J., Agalave, N. M. and Svensson, C. I. (2016). Pattern recognition receptors in chronic pain: Mechanisms and therapeutic implications. *Eur J Pharmacol* **788**, 261-73.

Ke, X., Jin, G., Yang, Y., Cao, X., Fang, R., Feng, X. and Lei, B. (2015). Synovial Fluid HMGB-1 Levels are Associated with Osteoarthritis Severity. *Clin Lab* **61**, 809-18.

Khomula, E. V., Viatchenko-Karpinski, V. Y., Borisyuk, A. L., Duzhyy, D. E., Belan, P. V. and Voitenko, N. V. (2013). Specific functioning of Cav3.2 T-type calcium and TRPV1 channels under different types of STZ-diabetic neuropathy. *Biochim Biophys Acta* **1832**, 636-49.

Koivisto, A., Hukkanen, M., Saarnilehto, M., Chapman, H., Kuokkanen, K., Wei, H., Viisanen, H., Akerman, K. E., Lindstedt, K. and Pertovaara, A. (2012). Inhibiting TRPA1 ion channel reduces loss of cutaneous nerve fiber function in diabetic animals: sustained activation of the TRPA1 channel contributes to the pathogenesis of peripheral diabetic neuropathy. *Pharmacol Res* **65**, 149-58.

Krzisch, M., Temprana, S. G., Mongiat, L. A., Armida, J., Schmutz, V., Virtanen, M. A., Kocher-Braissant, J., Kraftsik, R., Vutskits, L., Conzelmann, K. K. et al. (2015). Pre-existing astrocytes form functional perisynaptic processes on neurons generated in the adult hippocampus. *Brain Struct Funct* **220**, 2027-42.

Lam, D., Momeni, Z., Theaker, M., Jagadeeshan, S., Yamamoto, Y., Ianowski, J. P. and Campanucci, V. A. (2018). RAGE-dependent potentiation of TRPV1 currents in sensory neurons exposed to high glucose. *PLoS One* **13**, e0193312.

Maeda, T., Ozaki, M., Kobayashi, Y., Kiguchi, N. and Kishioka, S. (2013). HMGB1 as a potential therapeutic target for neuropathic pain. *J Pharmacol Sci* **123**, 301-5.

Mandadi, S., Tominaga, T., Numazaki, M., Murayama, N., Saito, N., Armati, P. J., Roufogalis, B. D. and Tominaga, M. (2006). Increased sensitivity of desensitized TRPV1 by PMA occurs through PKCepsilon-mediated phosphorylation at S800. *Pain* **123**, 106-16.

Marwaha, L., Bansal, Y., Singh, R., Saroj, P., Bhandari, R. and Kuhad, A. (2016). TRP channels: potential drug target for neuropathic pain. *Inflammopharmacology* **24**, 305-317.

Masuoka, T., Kudo, M., Yamashita, Y., Yoshida, J., Imaizumi, N., Muramatsu, I., Nishio, M. and Ishibashi, T. (2017). TRPA1 Channels Modify TRPV1-Mediated Current Responses in Dorsal Root Ganglion Neurons. *Front Physiol* **8**, 272.

Mohammadi-Farani, A., Ghazi-Khansari, M. and Sahebgharani, M. (2014). Glucose concentration in culture medium affects mRNA expression of TRPV1 and CB1 receptors and changes capsaicin toxicity in PC12 cells. *Iran J Basic Med Sci* **17**, 673-378.

Na Pombejra, S., Salemi, M., Phinney, B. S. and Gelli, A. (2017). The Metalloprotease, Mpr1, Engages AnnexinA2 to Promote the Transcytosis of Fungal Cells across the Blood-Brain Barrier. *Front Cell Infect Microbiol* **7**, 296.

Nakamura, Y., Morioka, N., Abe, H., Zhang, F. F., Hisaoka-Nakashima, K., Liu, K., Nishibori, M. and Nakata, Y. (2013). Neuropathic pain in rats with a partial sciatic nerve ligation is alleviated by intravenous injection of monoclonal antibody to high mobility group box-1. *PLoS ONE* **8**, e73640.

Newberry, K., Wang, S., Hoque, N., Kiss, L., Ahlijanian, M. K., Herrington, J. and Graef, J. D. (2016). Development of a spontaneously active dorsal root ganglia assay using multiwell multielectrode arrays. *J Neurophysiol* **115**, 3217-28.

Nishida, T., Tsubota, M., Kawaishi, Y., Yamanishi, H., Kamitani, N., Sekiguchi, F., Ishikura, H., Liu, K., Nishibori, M. and Kawabata, A. (2016). Involvement of high mobility group box 1 in the development and maintenance of chemotherapy-induced peripheral neuropathy in rats. *Toxicology* **365**, 48-58.

Obrosova, I. G. (2009). Diabetic painful and insensate neuropathy: pathogenesis and potential treatments. *Neurotherapeutics* **6**, 638-47.

Pabbidi, R. M., Yu, S. Q., Peng, S., Khardori, R., Pauza, M. E. and Premkumar, L. S. (2008). Influence of TRPV1 on diabetes-induced alterations in thermal pain sensitivity. *Mol Pain* **4**, 9.

Pawson, E. J., Duran-Jimenez, B., Surosky, R., Brooke, H. E., Spratt, S. K., Tomlinson, D. R. and Gardiner, N. J. (2010). Engineered zinc finger protein-mediated VEGF-a activation restores deficient VEGF-a in sensory neurons in experimental diabetes. *Diabetes* **59**, 509-18.

Pineau, P., Marchio, A., Terris, B., Mattei, M. G., Tu, Z. X., Tiollais, P. and Dejean, A. (1996). A t(3;8) chromosomal translocation associated with hepatitis B virus intergration involves the carboxypeptidase N locus. *J Virol* **70**, 7280-4.

Price, T. J. and Flores, C. M. (2007). Critical evaluation of the colocalization between calcitonin gene-related peptide, substance P, transient receptor potential vanilloid subfamily type 1 immunoreactivities, and isolectin B4 binding in primary afferent neurons of the rat and mouse. *J Pain* **8**, 263-72.

Radu, B. M., Iancu, A. D., Dumitrescu, D. I., Flonta, M. L. and Radu, M. (2013). TRPV1 properties in thoracic dorsal root ganglia neurons are modulated by intraperitoneal capsaicin administration in the late phase of type-1 autoimmune diabetes. *Cell Mol Neurobiol* **33**, 187-96.

Rami, H. K., Thompson, M., Stemp, G., Fell, S., Jerman, J. C., Stevens, A. J., Smart, D., Sargent, B., Sanderson, D., Randall, A. D. et al. (2006). Discovery of SB-705498: a potent, selective and orally bioavailable TRPV1 antagonist suitable for clinical development. *Bioorg Med Chem Lett* **16**, 3287-91.

Ristoiu, V., Shibasaki, K., Uchida, K., Zhou, Y., Ton, B. H., Flonta, M. L. and Tominaga, M. (2011). Hypoxia-induced sensitization of transient receptor potential vanilloid 1 involves activation of hypoxia-inducible factor-1 alpha and PKC. *Pain* **152**, 936-45.

Saleh, A., Smith, D. R., Tessler, L., Mateo, A. R., Martens, C., Schartner, E., Van der Ploeg, R., Toth, C., Zochodne, D. W. and Fernyhough, P. (2013). Receptor for advanced glycation end-products (RAGE) activates divergent signaling pathways to augment neurite outgrowth of adult sensory neurons. *Exp Neurol* **249**, 149-59.

Schindelin, J., Arganda-Carreras, I., Frise, E., Kaynig, V., Longair, M., Pietzsch, T., Preibisch, S., Rueden, C., Saalfeld, S., Schmid, B. et al. (2012). Fiji: an open-source platform for biological-image analysis. *Nat Methods* **9**, 676-82.

Shirley, S. H., von Maltzan, K., Robbins, P. O. and Kusewitt, D. F. (2014). Melanocyte and melanoma cell activation by calprotectin. *J Skin Cancer* **2014**, 846249.

Singh, V. P., Bali, A., Singh, N. and Jaggi, A. S. (2014). Advanced glycation end products and diabetic complications. *Korean J Physiol Pharmacol* **18**, 1-14.

Stanojlovic, M., Gusevac, I., Grkovic, I., Mitrovic, N., Zlatkovic, J., Horvat, A. and Drakulic, D. (2016). Repeated Estradiol Treatment Attenuates Chronic Cerebral Hypoperfusion-Induced Neurodegeneration in Rat Hippocampus. *Cell Mol Neurobiol* **36**, 989-99.

Staruschenko, A., Jeske, N. A. and Akopian, A. N. (2010). Contribution of TRPV1-TRPA1 interaction to the single channel properties of the TRPA1 channel. *J Biol Chem* **285**, 15167-77.

Tafesse, L., Sun, Q., Schmid, L., Valenzano, K. J., Rotshteyn, Y., Su, X. and Kyle, D. J. (2004). Synthesis and evaluation of pyridazinylpiperazines as vanilloid receptor 1 antagonists. *Bioorg Med Chem Lett* **14**, 5513-9.

Tomlinson, D. R. and Gardiner, N. J. (2008). Glucose neurotoxicity. *Nat Rev Neurosci* **9**, 36-45.

Wan, W., Cao, L., Khanabdali, R., Kalionis, B., Tai, X. and Xia, S. (2016). The Emerging Role of HMGB1 in Neuropathic Pain: A Potential Therapeutic Target for Neuroinflammation. *J Immunol Res* **2016**, 6430423.

Wang, S., Joseph, J., Ro, J. Y. and Chung, M. K. (2015). Modality-specific mechanisms of protein kinase C-induced hypersensitivity of TRPV1: S800 is a polymodal sensitization site. *Pain* **156**, 931-41.

Wang, Z. Y., McDowell, T., Wang, P., Alvarez, R., Gomez, T. and Bjorling, D. E. (2014). Activation of CB1 inhibits NGF-induced sensitization of TRPV1 in adult mouse afferent neurons. *Neuroscience* **277**, 679-89.

Wei, H., Hamalainen, M. M., Saarnilehto, M., Koivisto, A. and Pertovaara, A. (2009). Attenuation of mechanical hypersensitivity by an antagonist of the TRPA1 ion channel in diabetic animals. *Anesthesiology* **111**, 147-54.

Xiong, X., Gu, L., Wang, Y., Luo, Y., Zhang, H., Lee, J., Krams, S., Zhu, S. and Zhao, H. (2016). Glycyrrhizin protects against focal cerebral ischemia via inhibition of T cell activity and HMGB1-mediated mechanisms. *J Neuroinflammation* **13**, 241.

Yusaf, S. P., Goodman, J., Gonzalez, I. M., Bramwell, S., Pinnock, R. D., Dixon, A. K. and Lee, K. (2001). Streptozocin-induced neuropathy is associated with altered expression of voltage-gated calcium channel subunit mRNAs in rat dorsal root ganglion neurones. *Biochem Biophys Res Commun* **289**, 402-6.

Zhang, X., Yuan, Y., Jiang, L., Zhang, J., Gao, J., Shen, Z., Zheng, Y., Deng, T., Yan, H., Li, W. et al. (2014). Endoplasmic reticulum stress induced by tunicamycin and thapsigargin protects against transient ischemic brain injury: Involvement of PARK2-dependent mitophagy. *Autophagy* **10**, 1801-13.

Zhuang, Z. Y., Xu, H., Clapham, D. E. and Ji, R. R. (2004). Phosphatidylinositol 3-kinase activates ERK in primary sensory neurons and mediates inflammatory heat hyperalgesia through TRPV1 sensitization. *J Neurosci* **24**, 8300-9.

Zochodne, D. W. (2014). Mechanisms of diabetic neuron damage: Molecular pathways. *Handb Clin Neurol* **126**, 379-99.

Figures

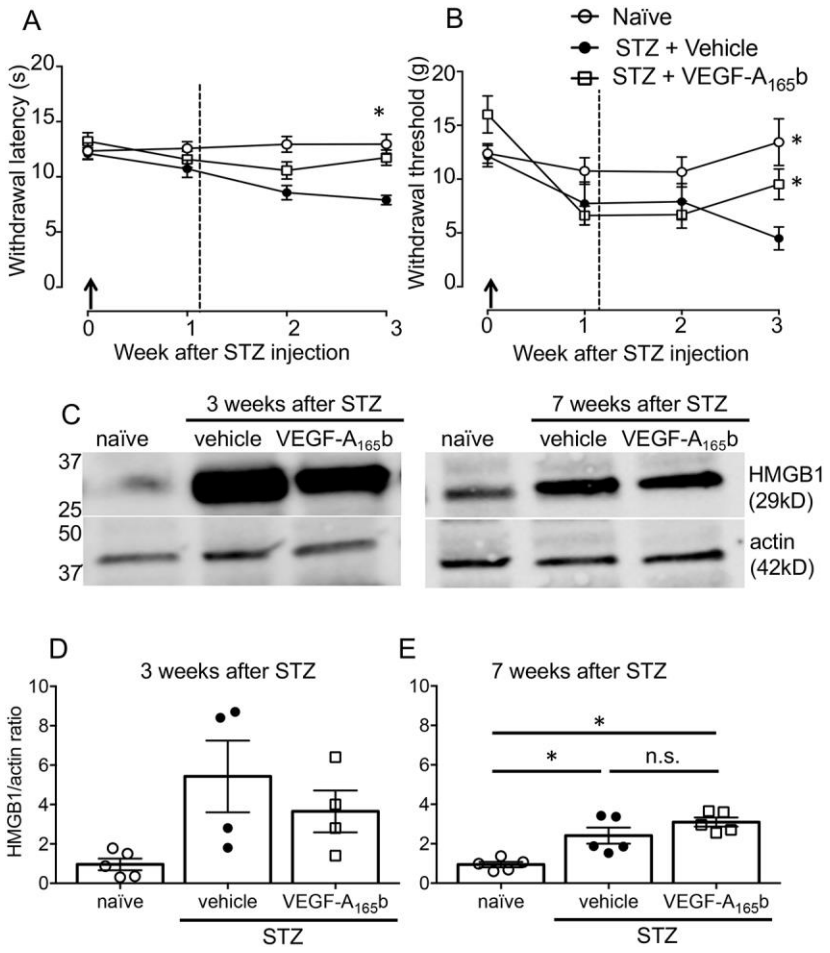

Figure 1. **Effect of VEGF-A$_{165}$b on thermal and mechanical hypersensitivity in STZ-diabetic rats**. A. STZ-induced thermal hypersensitivity was evident at 3 weeks after STZ injection, and was prevented with systemic VEGF-A$_{165}$b (2 way ANOVA, treatment: $F(2,103)=17.26$, $p= <0.0001$; time: $F(3,103)=3.74$, $p=0.013$; interaction: $F(6,103)=2.59$, $p = 0.022$. *$p<0.05$ post hoc Sidak's test). B. STZ-induced mechanical hypersensitivity, measured by a reduction in 50% withdrawal thresholds, and was prevented with VEGF-A$_{165}$b by week 3. (2 way ANOVA, treatment: $F(2,104)=6.744$, $p=0.0018$; , time: $F(3,104)=8.337$,$p=<0.0001$; interaction: $F(6,104)=3.03$, $p=0.009$. *$p<0.05$ post hoc Sidak's test). Arrows indicate STZ injection and the dotted line the start of bi-weekly systemic rhVEGF-A$_{165}$b or vehicle treatment. Data shown are mean ± SEM, naïve n=11

STZ + PBS n=9 STZ + VEGF-A_{165}b n=9. C. Representative Western blots of HMGB1 and actin in hind paw plantar skin at 3 and 7 weeks after STZ injection. D. HMGB1 protein expression was increased in skin from diabetic rats at both 3 (Kruskal-Wallis statistic 7.367, p=0.0132) and (E) 7 weeks (one way ANOVA F(2,12) =15.31, p=0.0005). The change in HMGB1 was not altered with VEGF-A_{165}b treatment. Plots show mean ± SEM and individual data points, n=5 (naïve at both 3 and 7 weeks, STZ 7 weeks), n=4 (STZ, 3 weeks. * p<0.05, n.s. not significant, post=hoc Dunn's (3 weeks) and Sidak's tests (7 weeks)).

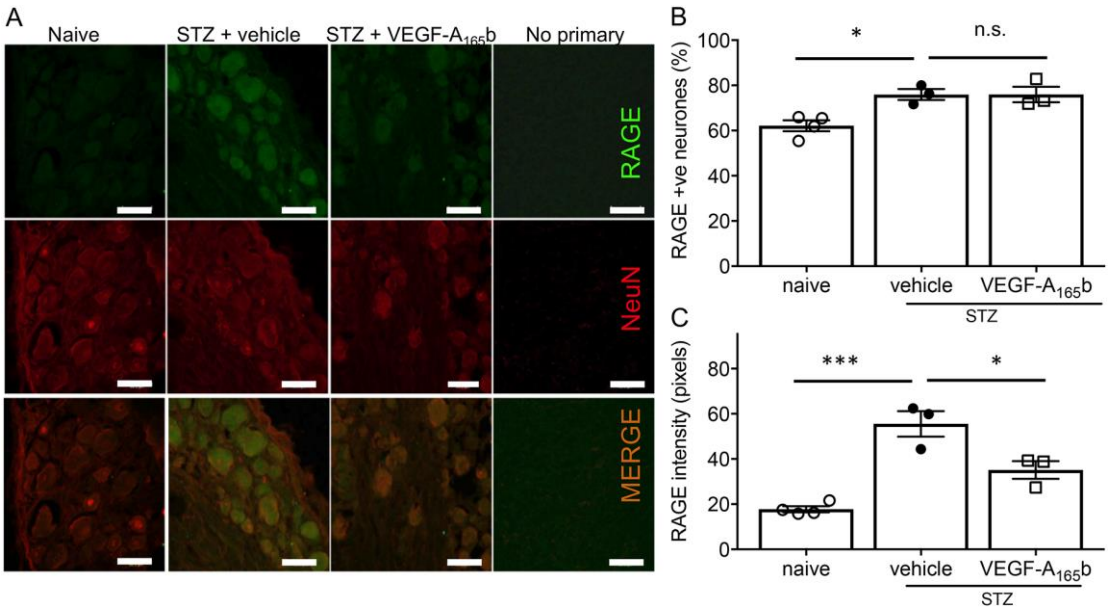

Figure 2. **RAGE is expressed in normal DRG neurons and is increased in STZ diabetic rats.**

A. Representative images of RAGE (green) and NeuN (neuronal marker, red) staining, showing RAGE expression in DRG neurons in naïve and diabetic rats. B. The percentage of the total neurons in the DRG expressing RAGE increased in diabetic rats, and this was not affected by VEGF-A_{165}b treatment (one way ANOVA $F(2,7)=9.104$, $p=0.0113$). C. RAGE intensity per neuron was increased in diabetic rats, and this increase was partially prevented by VEGF-A_{165}b treatment (one way ANOVA $F(2,7)=28.37$, $p=0.0004$,). Plots show mean ± SEM and individual data points, n= 4 (naïve) and 3 (all STZ groups). *$p<0.05$, ***$p<0.001$, n.s. = not significant, ANOVA + post-hoc Sidak's test.

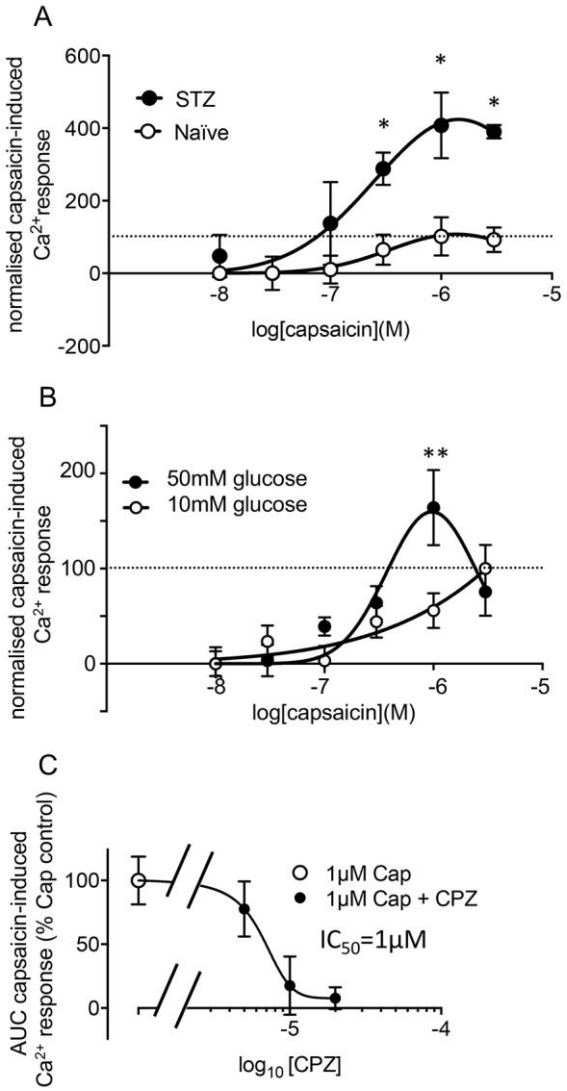

Figure 3. **STZ diabetes *in vivo*, and high glucose conditions *in vitro*, increase TRPV1 activity to agonist in DRG neurons.** A. Capsaicin evoked TRPV1 activity was greater in DRG neurons from diabetic rats (n=3) 3 weeks after STZ injection compared to DRG from naïve rats (n=4) (2 way ANOVA: interaction $F(5,28)=2.86$, $p=0.03$; capsaicin concentration $F(5,28)=8.45$, $p<0.0001$; STZ/naïve $F(1,28)=29.19$, $p<0.0001$. *$p<0.05$ post hoc Sidak's test). B. Capsaicin-evoked TRPV1 activity was also enhanced in naïve DRG neurons exposed to 24 h of 50mM glucose (n=5) compared to 10mM glucose for 24h (n=5, data shown are mean ± SEM, two way ANOVA interaction

F(5,149)=2.742, p=0.02; glucose concentration F(1,149)=2.45, p=0.12; capsaicin concentration F(2, 149)=8.16, p<0.0001) **p<0.01 post hoc Sidak's test. C. Capsaicin-evoked increase in intracellular calcium is blocked by TRPV1 antagonist capsazepine (n=7 replicates. (1μM Cap), 5 (1μM Cap + 5μM CPZ), and 8 (1μM Cap + 10 & 20μM CPZ. Neurons derived from 3 rats). Values are normalized to the maximum response evoked in the control conditions for each experiment (indicated by horizontal dashed line in A & B).

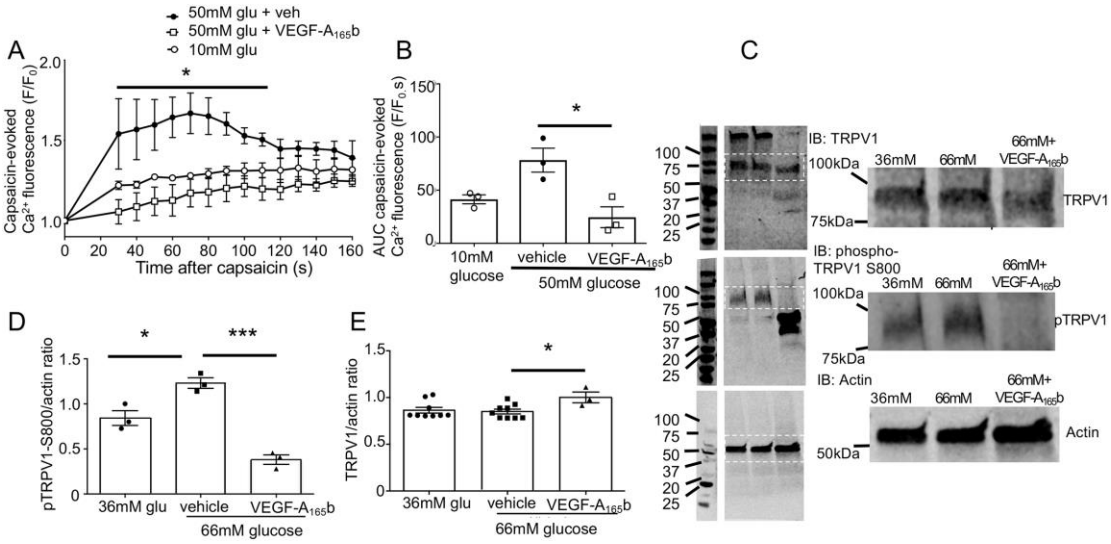

Figure 4. **VEGF-A$_{165}$b blocks high glucose-mediated TRPV1 sensitization and phosphorylation in DRG neurons**.

A. Capsaicin-evoked TRPV1 activity was enhanced in primary DRG neurons cultured in 50mM glucose and this was prevented with VEGF-A$_{165}$b co-treatment (n=3 per treatment, 2 way ANOVA interaction $F(28,90) = 1.081$ (ns), treatment $F(2,90)= 67.05$, $p<0.0001$, time $F(14, 90)= 3.842$, $p<0.0001$, *$p<0.05$ vehicle cf. VEGF-A$_{165}$b post hoc Tukey's test). B. Total capsaicin-evoked activity (AUC) was increased in high glucose conditions and reduced by VEGF-A$_{165}$b (1 way ANOVA $F(2,6)=9.424$, $p=0.014$ *$p<0.05$ post hoc Sidak's test). C. Representative Western blots for TRPV1 (96kD), pS800 TRPV1 (95kD), and actin (42kD) in 50B11 DRG neurons treated for 24h in basal glucose (36mM + 30mM mannitol), high glucose (66mM) ± VEGF-A$_{165}$b treatment (intervening lanes between markers and samples removed for clarity). D. Phosphorylated TRPV1 protein levels in 50B11 neurons increased in high glucose conditions compared to basal glucose conditions, and this was prevented with VEGF-A$_{165}$b treatment (n=3 per treatment 1 way ANOVA $F(2,6)=42.01$ $p<0.0003$, *$p<0.05$, ***$p<0.001$ post hoc Sidak's test). E. TRPV1

protein levels in 50B11 neurons were slightly increased in high glucose + VEGF-A_{165}b (one way ANOVA $F(2,18)=3.637$, $p=0.047$, $n=9$ in 36mM glucose & 66mM glucose + vehicle, $n=3$ for 66mM glucose + VEGF-A_{165}b as shown, *$p<0.05$ post hoc Sidak's test). Data shown are mean ± SEM, plus individual data points in B, D & E. (Please see methods text for different glucose concentrations in 50B11 and primary DRG neuronal cultures).

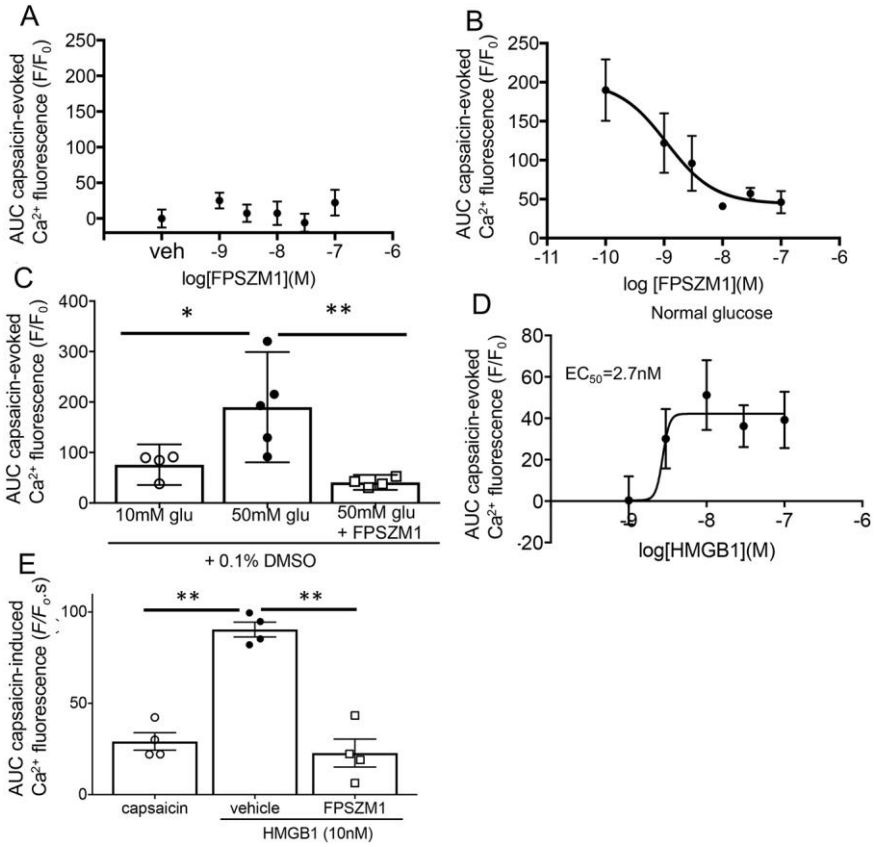

Figure 5. **RAGE agonism and antagonism modulate capsaicin-evoked intracellular calcium changes in DRG neurons**. A. FPSZM1 had no effect on capsaicin-evoked TRPV1 activity at any concentration in 10mM glucose conditions (n=4 per treatment). B. FPSZM1 significantly reduced the capsaicin-evoked TRPV1 activity in 50mM glucose conditions, in a concentration dependent manner (n=4 per treatment). C. The high glucose-induced increase in TRPV1 activity was completely prevented when neurons were co-treated with 10nM FPSZM1 (n=4, 10mM glucose and 50mM glucose + FPSZM1, n=5, 50mM glucose) (one way ANOVA $F(2,10)=8.398$, $p=0.0072$. *$p<0.05$, **$p<0.01$ post hoc Sidak's test). D. HMGB1 increased the capsaicin-evoked TRPV1 activity in a concentration-dependent manner (one way ANOVA $F95,30) =2.688$, $p=0.04$. *$p<0.05$ post-hoc Bonferroni tests c.f.

control, n=6 per treatment). E. The HMGB1-mediated (10nM) increase in capsaicin-evoked TRPV1 activity was blocked by 10nM FPSZM1 (n=4 per treatment, one way ANOVA $F(2,9)=42.63$, $p<0.0001$).

Data are mean ± SEM and individual data points as shown. *$p<0.05$. **$p<0.01$ post-hoc Sidak's tests.

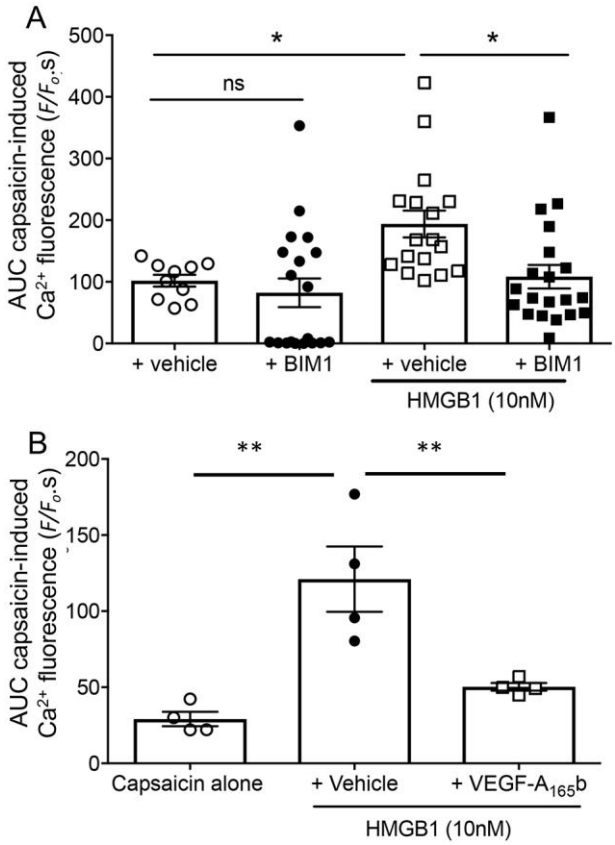

Figure 6. **HMGB1-mediated sensitization of capsaicin evoked TRPV1 activity is PKC-dependent.** A. BIM1 had no significant effect on capsaicin-evoked calcium response alone, but significantly reduced HMGB1-evoked responses (one way ANOVA F=5.627, DF=3, p=0.0018. *p<0.05 c.f. HMGB1+BIM1 and control post hoc Bonferroni tests. Capsaicin + vehicle n=10, capsaicin + BIM1 n=19, capsaicin + HMGB1 + vehicle n=17, capsaicin + HMGB1 + BIM1 n=20 as shown). B. VEGF-A_{165}b significantly reduced HMGB1-mediated sensitization of capsaicin-evoked TRPV1 activity (one way ANOVA F(2,9)=14.2, p=0.0016. **p<0.01 post-hoc Sidak's test). Data shown are mean ± SEM, n=4 per group.

Table 1. Antibody information

Target	Antibody type	Source and catalogue number	Dilution	Ref
Primary antibodies – Western blotting				
TRPV1	Rabbit polyclonal	Abcam (Ab10296)	1:500	(Hulse et al., 2014)
p800-TRPV1	Rabbit polyclonal	Abnova (PAB8499)	1:250	(Mandadi et al., 2006)
HMGB1	Rabbit polyclonal	Abcam (Ab18256)	1:1000	(Xiong et al., 2016)
Actin	Goat polyclonal	Santa Cruz (sc-1615)	1:200	(Stanojlovic et al., 2016)
Primary antibodies - immunofluorescence				
RAGE	Rabbit polyclonal	AbCam (Ab37647)	1:500	(Shirley et al., 2014)
NeuN	Mouse monoclonal	Millipore (MAB377)	1:200	(Krzisch et al., 2015)
Secondary antibodies – Western blotting				
Anti-rabbit	Donkey	Licor IRDye 680RD (926-68071)	1:1000	(Del Nagro et al., 2014)
Anti-goat	Donkey	Licor IRDye 800CW (925-32214)	1:1000	(Genead et al., 2012)
Secondary antibodies - immunofluorescence				
Anti-rabbit	Donkey	Alexa Fluor 488-conjugated (AbCam Ab150073)	1:500	(Zhang et al., 2014)
Anti-mouse	Chicken	Alexa Fluor 555-conjugated (AbCam150114)	1:500	(Na Pombejra et al., 2017)

Table S1. Representative data and effect sizes for outcome measures shown in the text.

Effect sizes calculated using G*Power (Faul et al., 2007).

Parameter Diabetic rat experiments	Naïve/control Mean±SD (n)	Diabetic Mean±SD(n)	Diabetic+VEGF-A_{165}b Mean±SD (n)	Effect size (n) (Cohen's d)	Figure
Behaviour - thermal	12.9 ± 2.9 (11)	7.9 ± 1.2 (9)	11.7 ±2.1 (9)	1.05 (28)	1
Behaviour – von Frey	13.4 ±7.2 (11)	4.5 ± 3.2 (9)	9.5 ± 4.3 (9)	0.74 (29)	1
HMGB1 western blots	0.96±0.7 (5)	5.4 ± 3.6 (4)	3.7 ± 2.1 (4)	0.94 (13)	2B
RAGE expression-%	62 ± 4.8 (4)	76 ± 4.1 (3)	76 ± 5.9 (3)	1.37 (11)	3B
RAGE expression-intensity	17.8 ± 2.7 (4)	55.6 ± 9.7 (3)	35.2 ± 6.7 (3)	2.6 (11)	3C
In vitro DRG/50B11 experiments	Control	Intervention (high glucose/ HMGB1)	Intervention + VEGF-A_{165}b/FPSZM1	Effect size (n)	Figure
TRPV1 activity (DRG neurons)	41.4 ± 7.3 (3)	78.3 ± 19.5 (3)	24.6 ± 17 (3)	1.32 (9)	5B
TRPV1 pTRPV1 (50B11 neurons)	0.86 ± 0.09 (9) 0.84 ± 0.14 (3)	0.85 ± 0.07 (9) 1.23 ±0.1 (3)	1.002 ± 0.09 (3) 0.38 ± 0.09 (3)	0.56 (21) 3.48 (9)	5E 5D
TRPV1 activity (+HMGB1)	29 ± 9.6 (4)	121 ± 43 (4)	50 ± 5 (4)	3.93 (12)	8B
TRPV1 activity (high glu ± FPSZM1)	75.8 ± 25 (4)	189.9 ± 88 (5)	40.9 ± 9.3 (4)	2.42 (13)	6C
TRPV1 activity (HMGB ± FPSZM1)	29.1±4.8 (4)	90.4±4.1 (4)	22.8±7.7 (4)	2.65 (12)	7B

Faul, F., Erdfelder, E., Lang, A. G. and Buchner, A. (2007). G*Power 3: a flexible statistical power analysis program for the social, behavioral, and biomedical sciences. *Behav Res Methods* 39, 175-91.

Figure S1

The antibody used for RAGE immunofluorescent staining of DRG neurons in Figure 2 was verified for specificity in immortalised rat DRG 50B11 neurons. This confirmed that the antibody detected a single band of size ~45kD. B= basal glucose (36mM), H = high glucose (66mM)